Separation Science and Technology
Publication details, including instructions for authors and subscription information:
http://www.informaworld.com/smpp/title~content=t713708471

Soil Cleanup by In-Situ Aeration. XXIII. Effect of Air Channeling

David J. Wilson[a]; José M. Rodríguez-Maroto[b]; César Gómez-Lahoz[b]
[a] DEPARTMENT OF CHEMISTRY, VANDERBILT UNIVERSITY, NASHVILLE, TENNESSEE, USA [b] DEPARTMENTO DE INGENIERÍA QUÍMICA, FACULTAD DE CIENCIAS, CAMPUS UNIVERSITARIO DE TEATINOSm UNIVERSIDAD DE MÁLAGA, MÁLAGA, SPAIN

To cite this Article Wilson, David J. , Rodríguez-Maroto, José M. and Gómez-Lahoz, César(1995) 'Soil Cleanup by In-Situ Aeration. XXIII. Effect of Air Channeling', Separation Science and Technology, 30: 12, 2491 — 2508

To link to this Article: DOI: 10.1080/01496399508021397

URL: http://dx.doi.org/10.1080/01496399508021397

SEPARATION SCIENCE AND TECHNOLOGY, **30**(12), pp. 2491–2508, 1995

Soil Cleanup by In-Situ Aeration. XXIII. Effect of Air Channeling

DAVID J. WILSON
DEPARTMENT OF CHEMISTRY
VANDERBILT UNIVERSITY
NASHVILLE, TENNESSEE 37235 USA

JOSÉ M. RODRÍGUEZ-MAROTO and CÉSAR GÓMEZ-LAHOZ
DEPARTAMENTO DE INGENIERÍA QUÍMICA
FACULTAD DE CIENCIAS
CAMPUS UNIVERSITARIO DE TEATINOS
UNIVERSIDAD DE MÁLAGA
29071 MÁLAGA, SPAIN

ABSTRACT

A distributed diffusion model for soil vapor extraction (SVE) is developed in which air advection occurs through conducting channels or tubes of high air permeability; volatile organic compound (VOC) is removed by diffusion from the surrounding porous medium to these channels, where it is removed by advection. The results obtained with this model are similar to those obtained with other distributed diffusion SVE models in that initial rapid VOC removal is followed by a rather rapid decrease in effluent soil gas VOC concentration and extended tailing of the cleanup. It is noted that soil gas VOC concentration rebound after SVE well shutdown provides useful information about the extent of cleanup only if the soil gas is recovered from the domain which was actually contaminated.

INTRODUCTION

Soil vapor extraction (SVE) provides a well-tested and widely accepted method for removing volatile organic compounds (VOCs) from the vadose zone at contaminated sites (Refs. 1–4, for example). The mathematical modeling of SVE gives insight into the physical and chemical factors governing the process, and provides assistance for initial site evaluation, design of pilot-scale field studies, interpretation of lab- and pilot-scale field data, design of full-field-scale operations, and estimation of costs and cleanup times. A summary of groups working on SVE modeling was given in an earlier paper (5).

Early SVE models made the assumption of local equilibrium between VOC concentrations in the mobile (advecting) gas phase and in the various stationary phases in the soil (adsorbed, dissolved in soil moisture, NAPL, etc.). In many cases this led to excessively optimistic predictions of the rate of remediation. Rapid decline in off-gas VOC concentrations after the first few days (or few hours), prolonged periods of tailing during the final phase of the cleanup, and soil gas VOC concentration rebound after well shutdown indicated that local equilibrium of VOC between phases was not being maintained and that release of VOC to the moving soil gas was impeded by slow diffusion and/or desorption processes. DiGiulio (6) discussed the impact of mass transport limitations in SVE, and field tests for the identification and assessment of such bottlenecks have been proposed (7).

Recently we explored various SVE models in which diffusion processes are handled by a distributed diffusion technique which permits one to obtain with the same parameter set the initial high off-gas VOC concentrations, the subsequent rapid fall-offs in off-gas VOC concentrations, and the prolonged tailings in the cleanups which are often observed (8–10). Other papers explored the effects of desorption rates and equilibria (5) and natural soil organic material (11) on the kinetics of SVE.

In the present paper we explore another physical picture of the diffusion process in soil vapor extraction, based on observations made in connection with the sparging of small-scale water-saturated sand beds. In that work we observed that the air bubbles rising to the surface of the zone of saturation appeared at locations which were quite persistent in time, indicating that the air was moving along preferred channels through the simulated aquifer rather than rising as discrete, independent, and random bubbles. This observation was used to develop a model for in-situ air sparging in which the air moved along preferred channels, and in which VOC was transported to the channels by diffusion and aqueous circulation (12). Here we extend the idea of air moving mainly along preferred channels to soil vapor extraction in the vadose zone. This is the sort of situation one might have if the soil is deeply cracked by drying from time to time, if the soil has been disturbed by nearby blasting, if there are animal burrows, or if there are rotted tree roots. All of these could provide extended high-conductivity pathways for air movement.

ANALYSIS

The well geometry selected is that of a single vertical well screened for a short length at the bottom. We assume that the vadose zone soil is homogeneous and isotropic, so that the method of images can be used to calculate the soil gas pressure and superficial velocity components in the domain of influence of the well. A diagram of the well and a representative volume element (in cylindrical coordinates r and z) is shown in Fig. 1.

The mean radius of the high-permeability channels which are assumed to conduct the advecting air in this model is taken to be a_{chan}, and the mean radius of the domains (assumed cylindrical) through which these channels pass is b. Let us focus on a single volume element ΔV_{ij}, for which

$$r_i = (i - 1)\Delta r \tag{1}$$

$$z_j = (j - 1)\Delta z \tag{2}$$

so that

$$\Delta V_{ij} = \pi(r_{i+1}^2 - r_i^2)\Delta z = \pi(2i - 1)(\Delta r)^2\Delta z \tag{3}$$

The number of channels in the volume element is then given by

$$n_{ij} = (\Delta V_{ij})/(\pi b^2 \Delta z) \tag{4}$$

We let n_r and n_z be the number of intervals in the r and z directions into

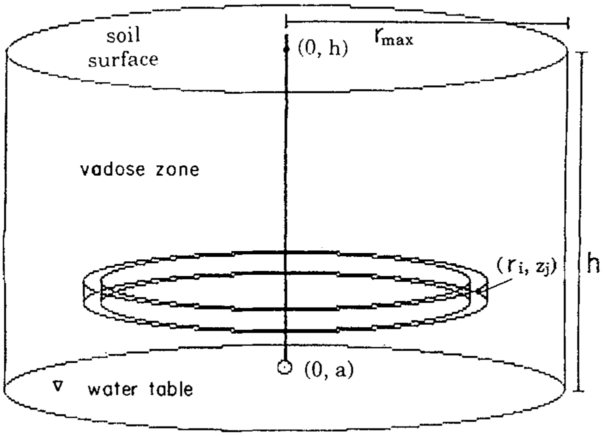

FIG. 1 Geometry and notation for the SVE well.

which the domain is divided; then $\Delta r = r_{\max}/n_r$ and $\Delta z = h/n_z$. The distribution of channels and their associated cylindrical domains within a segment of the volume element ΔV_{ij} is shown schematically in Fig. 2.

Diffusion of VOC to the Air Channels

Let us next examine one of the cylindrical domains and its associated air channel. See Fig. 3. The domain is partitioned into n_u annuli, each of thickness Δu, as indicated. Then

$$\Delta u = (b - a_{\text{chan}})/n_u \tag{5}$$

and the inner radius of the kth annulus is given by

$$u_k = a_{\text{chan}} + (k - 1)\Delta u \tag{6}$$

The volume of the kth annulus is given by

$$\Delta v_k = \pi \Delta z(u_{k+1}^2 - u_k^2) = \pi \Delta z[2a_{\text{chan}}\Delta u + (2k - 1)(\Delta u)^2] \tag{7}$$

Let

σ = air-filled porosity in the domain surrounding the air channel
ω = water-filled porosity in the domain surrounding the air channel

We assume that VOC is present in this domain in aqueous solution and in the vapor phase, and that these are at local equilibrium with respect to VOC transport within any given annulus in the domain. Define

$$C_{ijk}^s = \sigma C_{ijk}^g + \omega C_{ijk}^w \tag{8}$$

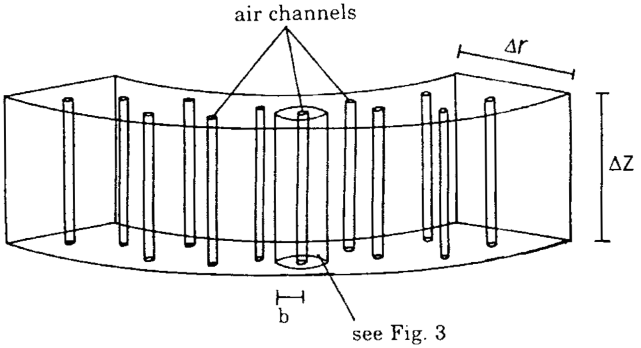

FIG. 2 A segment of a volume element showing the high-permeability air channels.

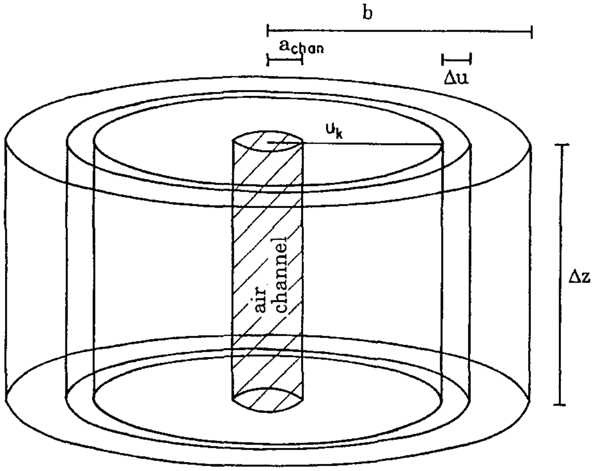

FIG. 3 An air channel and the surrounding porous low-permeability domain.

where

C^g_{ijk} = vapor phase VOC concentration in the *k*th annuli of the domains in ΔV_{ij}, kg/m^3 of the vapor phase
C^w_{ijk} = aqueous phase VOC concentration in the *k*th annuli of the domains in ΔV_{ij}, kg/m^3 of the aqueous phase
C^s_{ijk} = total VOC concentration in the *k*th annuli of the domains in ΔV_{ij}, kg/m^3 of the porous medium

From Henry's law we have

$$C^g_{ijk} = K_H C^w_{ijk} \tag{9}$$

which, with Eq. (8), gives after rearrangement

$$C^g_{ijk} = \frac{K_H C^s_{ijk}}{\sigma K_H + \omega} \tag{10}$$

Unless the domains are nearly saturated with water, the overwhelming bulk of the diffusion transport of VOC in them will take place in the gas phase. Since, however, the C^g_{ijk} and the C^s_{ijk} are proportional, we can write the diffusion transport equations in terms of the C^s_{ijk} and an effective diffusion constant *D* which includes the proportionality constant $K_H/(\sigma K_H + \omega)$, as well as terms including the tortuosity, the degree of water saturation of the medium, etc. Then

$$\Delta v_k \frac{dC^s_{ijk}}{dt} = \frac{2\pi \Delta z D}{\Delta u} [u_k(C^s_{i,j,k-1} - C^s_{ijk}) + u_{k+1}(C^s_{i,j,k+1} - C^s_{ijk})],$$

$$k = 2, 3, \ldots, n_u - 1 \quad (11)$$

and

$$\frac{dC^s_{ijk}}{dt} = \frac{2\pi \Delta z D}{\Delta v_k \Delta u} [u_k(C^s_{i,j,k-1} - C^s_{ijk}) + u_{k+1}(C^s_{i,j,k+1} - C^s_{ijk})],$$

$$k = 2, 3, \ldots, n_u - 1 \quad (12)$$

There is no mass transport through the outer surface of the outermost annulus, so

$$\frac{dC^s_{i,j,n_u}}{dt} = \frac{2\pi \Delta z D}{\Delta v_{n_u} \Delta u} u_{n_u}(C^s_{i,j,n_u-1} - C^s_{i,j,n_u}) \quad (13)$$

For the innermost annulus we assume that the concentration of VOC adjacent to its inner surface is in equilibrium with the gas phase VOC concentration in the high-permeability channel, C^g_{ij}. This yields

$$\frac{dC^s_{ij1}}{dt} = \frac{2\pi \Delta z D}{\Delta v_1 \Delta u} [2a_{\text{chan}}(C^g_{ij}/K'_{\text{H}} - C^s_{ij1}) + u_2(C^s_{ij2} - C^s_{ij1})] \quad (14)$$

where

$$K'_{\text{H}} = K_{\text{H}}/(\sigma K_{\text{H}} + \omega) \quad (15)$$

Movement of VOC in the Air Channels

The term describing diffusion of VOC into the air-conducting channels is obtained as follows. Let the air-filled porosity of the medium in these channels be σ_m, and recall that n_{ij} is the number of such channels in ΔV_{ij}. Then a partial mass balance on VOC in these channels including only diffusion transport gives

$$\sigma_m n_{ij} \pi a^2_{\text{chan}} \Delta z \left[\frac{\partial C^g_{ij}}{\partial t}\right]_{\text{diff}} = n_{ij} 2\pi a_{\text{chan}} \Delta z D \frac{(C^s_{ij1} - C^g_{ij}/K'_{\text{H}})}{\Delta u/2} \quad (16)$$

which simplifies to

$$\left[\frac{\partial C^g_{ij}}{\partial t}\right]_{\text{diff}} = \frac{4D}{\sigma_m a_{\text{chan}} \Delta u} (C^s_{ij1} - C^g_{ij}/K'_{\text{H}}) \quad (17)$$

The advection term is readily obtained and is as follows. Let the Inner, Outer, Top, and Bottom surface areas of the volume element ΔV_{ij} be given by

$$A_{ij}^{\mathrm{I}} = 2\pi(i - 1)\Delta r\Delta z \tag{18}$$

$$A_{ij}^{\mathrm{O}} = 2\pi i\Delta r\Delta z \tag{19}$$

$$A_{ij}^{\mathrm{T}} = A_{ij}^{\mathrm{B}} = \pi(2i - 1)(\Delta r)^2 \tag{20}$$

Let the superficial gas velocity components normal to these surfaces be given by

$$v_{ij}^{\mathrm{I}} = v_r[(i - 1)\Delta r, (j - 1/2)\Delta z] \tag{21}$$

$$v_{ij}^{\mathrm{O}} = v_r[i\Delta r, (j - 1/2)\Delta z] \tag{22}$$

$$v_{ij}^{\mathrm{T}} = v_z[(i - 1/2)\Delta r, j\Delta z] \tag{23}$$

$$v_{ij}^{\mathrm{B}} = v_z[(i - 1/2)\Delta r, (j - 1)\Delta z] \tag{24}$$

Define

$$\begin{aligned} S(v) &= 1, \qquad v > 0 \\ &= 0, \qquad v \leq 0 \end{aligned} \tag{25}$$

Then

$$\begin{aligned} \left[\frac{\partial C_{ij}^g}{\partial t}\right]_{\mathrm{adv}} = \frac{1}{\sigma_m n_{ij} \pi a_{\mathrm{chan}}^2 \Delta z} &\{A_{ij}^{\mathrm{I}} v_{ij}^{\mathrm{I}}[S(v^{\mathrm{I}})C_{i-1,j}^g + S(-v^{\mathrm{I}})C_{ij}^g] \\ &+ A_{ij}^{\mathrm{O}} v_{ij}^{\mathrm{O}}[-S(-v^{\mathrm{O}})C_{i+1,j}^g - S(v^{\mathrm{O}})C_{ij}^g] \\ &+ A_{ij}^{\mathrm{B}} v_{ij}^{\mathrm{B}}[S(v^{\mathrm{B}})C_{i,j-1}^g + S(-v^{\mathrm{B}})C_{ij}^g] \\ &+ A_{ij}^{\mathrm{T}} v_{ij}^{\mathrm{T}}[-S(-v^{\mathrm{T}})C_{i,j+1}^g - S(v^{\mathrm{T}})C_{ij}^g]\} \end{aligned} \tag{26}$$

Here $S(v^{\mathrm{I}})$ is an abbreviation for $S(v_{ij}^{\mathrm{I}})$, etc.

The superficial gas velocity field is calculated as was done previously (Ref. 9, for example); we therefore only present the results. The velocity potential $W(r, z)$ is defined as

$$W = P^2(r, z) - P_a^2 \tag{27}$$

where P_a is the ambient pressure (1 atm) and $P(r, z)$ is the pressure at the point (r, z). Then

$$\begin{aligned} W = A \sum_{n=-\infty}^{\infty} \Bigg[&- \frac{1}{\{r^2 + [z - 4nh - a]^2\}^{1/2}} - \frac{1}{\{r^2 + [z - 4nh + a]^2\}^{1/2}} \\ &+ \frac{1}{\{r^2 + [z - (4n - 2)h - a]^2\}^{1/2}} + \frac{1}{\{r^2 + [z - (4n - 2)h + a^2\}^{1/2}} \Bigg] \end{aligned} \tag{28}$$

Here

$$A = \frac{P_w^2 - P_a^2}{S'} \tag{29}$$

where

$$P_w = \text{wellhead pressure, atm}$$

and

$$S' = \sum_{n=-\infty}^{\infty} \left[-\frac{1}{\{r_w^2 + [a - 4nh - a]^2\}^{1/2}} - \frac{1}{\{r_w^2 + [a - 4nh + a]^2\}^{1/2}} \right.$$

$$(30)$$

$$\left. + \frac{1}{\{r_w^2 + [a - (4n - 2)h - a]^2\}^{1/2}} + \frac{1}{\{r_w^2 + [a - (4n - 2)h + a]^2\}^{1/2}} \right]$$

The pressure is given by

$$P(r, z) = [P_a^2 + W(r, z)]^{1/2} \tag{31}$$

and the superficial gas velocity by

$$\mathbf{v} = -K_D \nabla P \tag{32}$$

where K_D, Darcy's constant, is given by

$$K_D = \frac{qS'}{2(P_w^2 - P_a^2)} \tag{33}$$

where q is the volumetric flow rate of the well (m^3/s) and the units of K_D are $m^2/\text{atm}\cdot\text{s}$.

From Eq. (27) we have

$$W = 2P\nabla P \tag{34}$$

This, with Eqs. (31) and (32), yields

$$\mathbf{v} = -\frac{K_D \nabla W}{2[W + P_a^2]^{1/2}} = v_r \mathbf{e}_r + v_z \mathbf{e}_z \tag{35}$$

where $\mathbf{e}_r$ and $\mathbf{e}_z$ are unit vectors in the r and z directions. The derivatives of W needed for the velocities are given by

$$\frac{\partial W}{\partial r} = A \sum_{n=-\infty}^{\infty} \left[\frac{r}{\{r^2 + [z - 4nh - a]^2\}^{3/2}} + \frac{r}{\{r^2 + [z - 4nh - a]^2\}^{3/2}} \right.$$

$$(36)$$

$$\left. - \frac{r}{\{r^2 + [z - (4n - 2)h - a]^2\}^{3/2}} - \frac{r}{\{r^2 + [z - (4n - 2)h + a]^2\}^{3/2}} \right]$$

and

$$\begin{aligned}\frac{\partial W}{\partial z} = A \sum_{n=-\infty}^{\infty} \Bigg[& \frac{z - 4nh - a}{\{r^2 + [z - 4nh - a]^2\}^{3/2}} + \frac{z - 4nh + a}{\{r^2 + [z - 4nh + a]^2\}^{3/2}} \\ & - \frac{z - (4n - 2)h - a}{\{r^2 + [z - (4n - 2)h - a]^2\}^{3/2}} - \frac{z - (4n - 2)h + a}{\{r^2 + [z - (4n - 2)h + a]^2\}^{3/2}} \Bigg]\end{aligned} \tag{37}$$

This completes the summary of the calculation of the soil gas velocity field.

Finally, the behavior of the C_{ij}^g is controlled by

$$\frac{dC_{ij}^g}{dt} = \left[\frac{\partial C_{ij}^g}{\partial t}\right]_{\text{diff}} + \left[\frac{\partial C_{ij}^g}{\partial t}\right]_{\text{adv}} \tag{38}$$

where the terms on the right-hand side of Eq. (38) are given by Eqs. (17) and (26). The C_{ijk}^s are governed by Eqs. (12), (13), and (14). The residual total mass of VOC in the region of interest at time t is given by

$$M(t) = \sum_{i=1}^{n_r} \sum_{j=1}^{n_z} n_{ij} \left\{ \left[\sum_{k=1}^{n_u} \Delta v_k C_{ijk}^s \right] + \sigma_m \pi a_{\text{chan}}^2 \Delta z C_{ij}^g \right\} \tag{39}$$

Soil gas VOC concentration rebound after SVE well shutdown can be followed by simply switching off the advection term in Eq. (38) and following the subsequent evolution of the C_{ij}^gs of interest.

RESULTS AND DISCUSSION

The model was implemented in TurboBASIC and runs were made on an MMG 386-DX microcomputer using MS-DOS and running at 33 MHz. A typical run required about 25 minutes. Default values of the model parameters are given in Table 1.

The effect of the radius b of the porous domains surrounding the air channels is shown in Fig. 4. As expected, the cleanup time increases dramatically with increasing domain radius as this variable increases from 10 to 30 cm. The total area of interface between these domains and the air channels decreases with increasing domain radius, and the length through which VOC must diffuse increases, so one expects a very strong dependence of cleanup time on domain radius. In these runs the gas flow rate is 100 cfm, and the SVE is very strongly diffusion-limited.

At a gas flow rate of 10 cfm (see Fig. 5) the process is not quite so strictly diffusion-limited, and the dependence of cleanup time on porous domain radius b is not as strong as was observed in Fig. 4. This depen-

TABLE 1
Default Values of the Parameters Used in the Model

Depth of vadose zone	8 m
Radius of domain of interest	6 m
Well depth	6.5 m
Radius of well gravel packing	0.15 m
Gas flow rate	100 cfm 0.04719 m^3/s
Wellhead pressure	0.85 atm
Soil density	1.7 g/cm^3
Stagnant air-filled porosity	0.25
Water-filled porosity	0.10
Radius of mobile air channels	1 cm
Mean distance between air channels	20 cm
Δr	1 m
Δz	1 m
Δt	450 seconds
n_u	5
Porosity of the mobile gas conduits	0.4
Henry's constant of VOC (trichloroethylene)	0.2821
Diffusion constant of VOC in the porous medium	2×10^{-8} m^2/s
Initial VOC concentration in contaminated domain	100 mg/kg
Radius of zone of contamination	6 m
Depth of zone of contamination	4 m

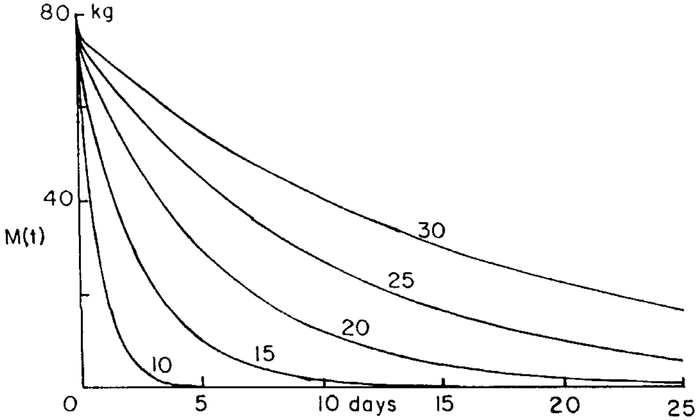

FIG. 4 Plots of total residual VOC mass $M(t)$ versus time; effect of the radius b of the porous low-permeability domains surrounding the air channels. b = 10 to 30 cm, as indicated; air flow rate = 100 cfm; other parameters as in Table 1.

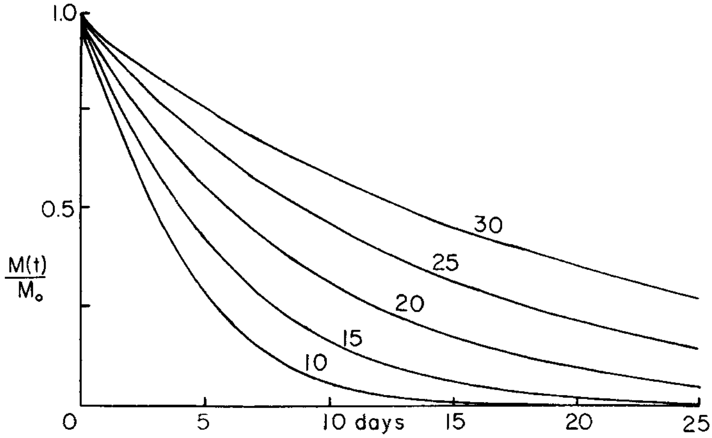

FIG. 5 Plots of normalized total residual VOC mass $M(t)/M_0$ versus time; effect of the radius b of the porous low-permeability domains surrounding the air channels. b = 10 to 30 cm, as indicated; air flow rate = 10 cfm; other parameters as in Table 1.

dence is still quite large, however, indicating that diffusion limitations are important for this set of runs, too.

The area of the interface between the air-conducting channels and the surrounding porous domains is proportional to the radius of the air channels, a_{chan}. Since diffusion transport to these channels must take place through this interface, we expect that SVE will be slowed down as a_{chan} is decreased. The results plotted in Fig. 6 indicate that this is the case, and that the effect is strong under diffusion-limited conditions.

When diffusion processes are limiting, the effect of the Henry's constant of the VOC is relatively small, as seen in Fig. 7. The moving gas is far from equilibrium with the stationary aqueous and vapor phases for these runs, although we see some significant reduction in cleanup rate as K_H is reduced from .01 to .005.

The effect of the depth to which the contamination extends below the surface of the soil is shown in Figs. 8 (gas flow rate = 100 cfm, domain radius = 6 m) and 9 (gas flow rate = 10 cfm, domain radius = 10 m). Interestingly, the domains contaminated to a depth of 8 m cleaned up slightly more rapidly than those contaminated to a depth of 4 m, probably because of the rapid movement of air laterally in toward the well through the deeper contaminated material near the well.

The effect of gas flow rate on SVE cleanup rate is shown in Fig. 10 (radius of contaminated domain = 6 m, gas flow rates = 10 and 100 cfm)

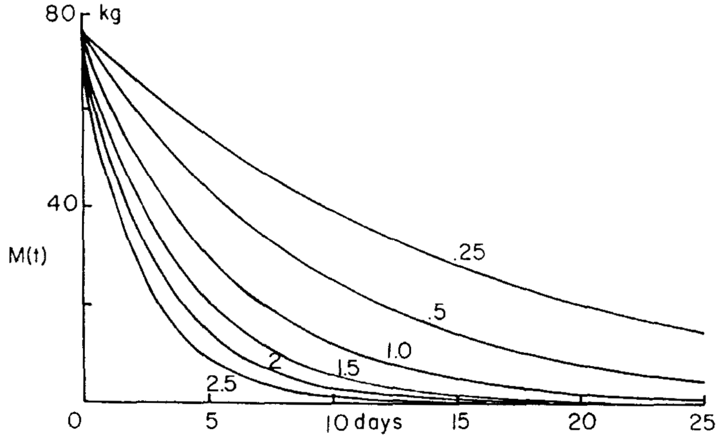

FIG. 6 Plots of total residual VOC mass $M(t)$ versus time; effect of the radius a_{chan} of the high-permeability air channels. a_{chan} = 0.25, 0.5, 1.0, 1.5, 2.0, and 2.5 cm as indicated. Other parameters as in Table 1.

and Fig. 11 (radius of contaminated domain = 14 m, gas flow rates = 10 and 100 cfm). For the smaller domain (Fig. 10), SVE is strongly diffusion-limited at both gas flow rates, and the two curves are quite similar. In Fig. 10 the higher flow rate initially gives some advantage, but this diminishes as the cleanup progresses; this is the result of the initial rapid release

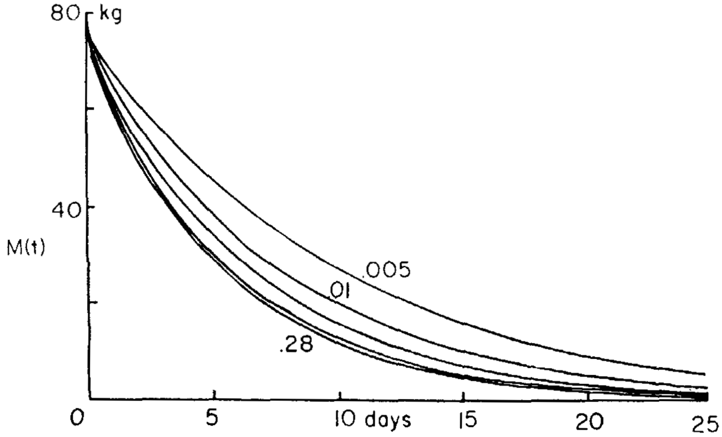

FIG. 7 Plots of total residual VOC mass $M(t)$ versus time; effect of the Henry's constant of the VOC. K_H = 0.2821, 0.1, 0.02, 0.01, and 0.005 (dimensionless) from the bottom up; other parameters as in Table 1.

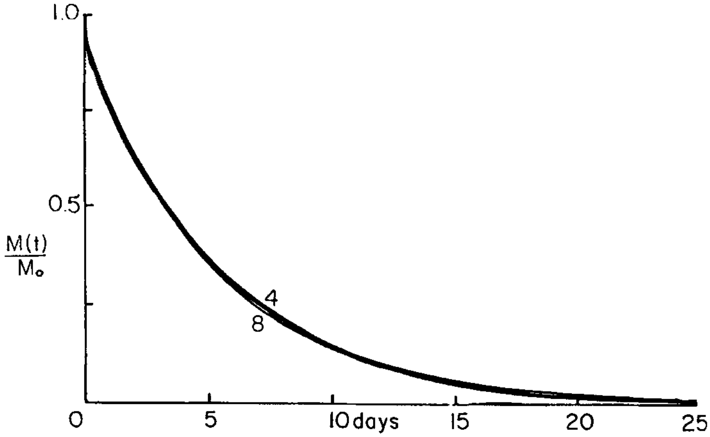

FIG. 8 Plots of normalized total residual VOC mass $M(t)/M_0$ versus time; effect of depth d_{contam} to which contamination extends. From the bottom up, $d_{\text{contam}} = 8$, 6, and 4 m; gas flow rate = 100 cfm; other parameters as in Table 1.

of VOC by diffusion. This phenomenon could not be reproduced by a lumped parameter model. For the larger domain the gas flow rate in the peripheral regions is evidently sufficiently slow that SVE is no longer diffusion-limited in those regions, so gas flow rate has a stronger effect on cleanup time.

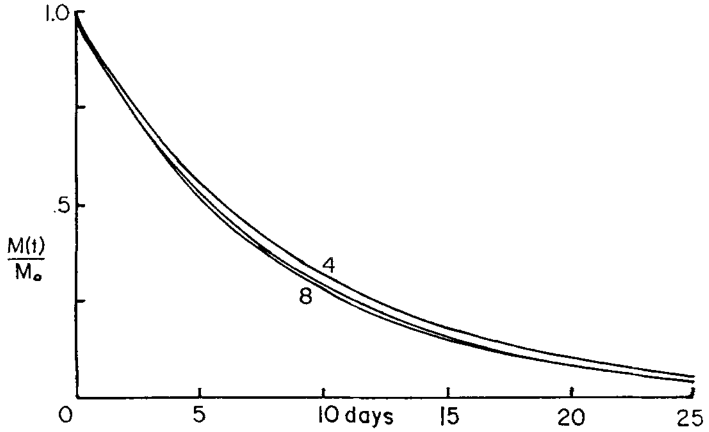

FIG. 9 Plots of normalized total residual VOC mass $M(t)/M_0$ versus time; effect of depth d_{contam} to which contamination extends. From the bottom up, $d_{\text{contam}} = 8$, 6, and 4 m; gas flow rate = 10 cfm; other parameters as in Table 1.

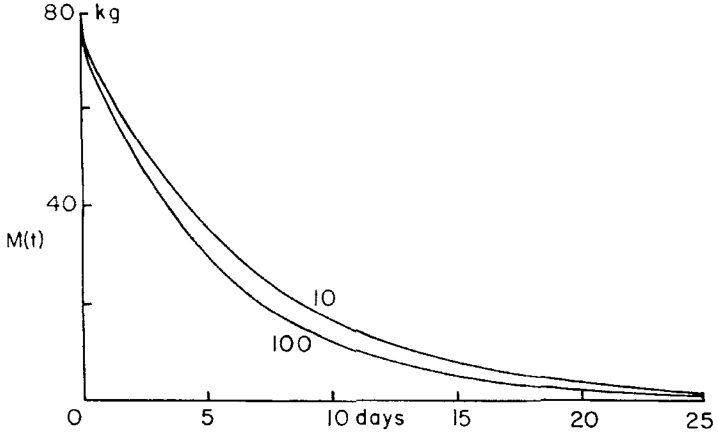

FIG. 10 Plots of total residual VOC mass $M(t)$ versus time; effect of gas flow rate q. q = 10 and 100 cfm as indicated; radius of contamination = 6 m; other parameters as in Table 1.

Figures 12, 13, and 14 show soil gas VOC concentration rebound after the SVE well has been operated for some days and then shut down. The usual process is that VOC continues to be released from the soil matrix by diffusion, but is no longer removed by advecting soil gas, so the VOC concentration in the gas phase increases with time after shutdown. The

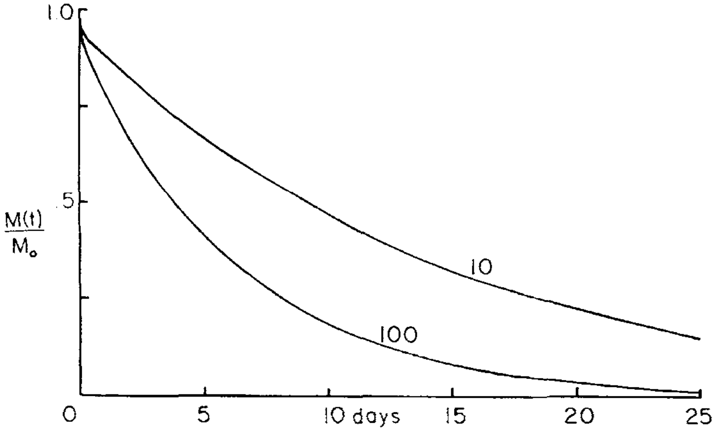

FIG. 11 Plots of total residual VOC mass $M(t)$ versus time; effect of gas flow rate q. q = 10 and 100 cfm as indicated; radius of contamination = 14 m; other parameters as in Table 1.

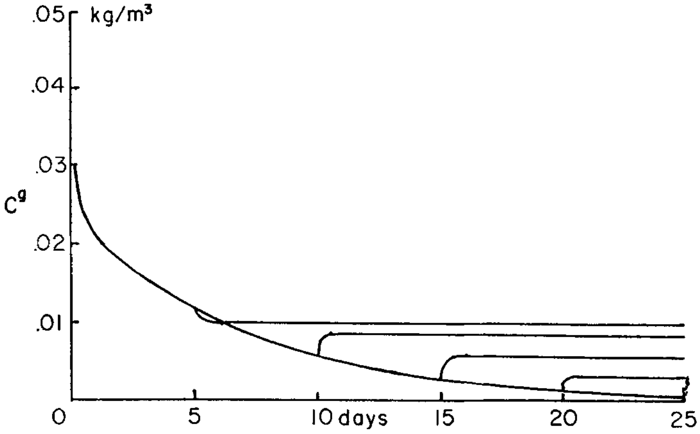

FIG. 12 Plots of vapor phase VOC concentration adjacent to the SVE well; rebound after well shutdown. Gas flow rate = 10 cfm; other parameters as in Table 1. The curves branching off from the descending curve show VOC concentration rebound after periods of well operation of 5, 10, 15, and 20 days. The well lies below the contaminated zone.

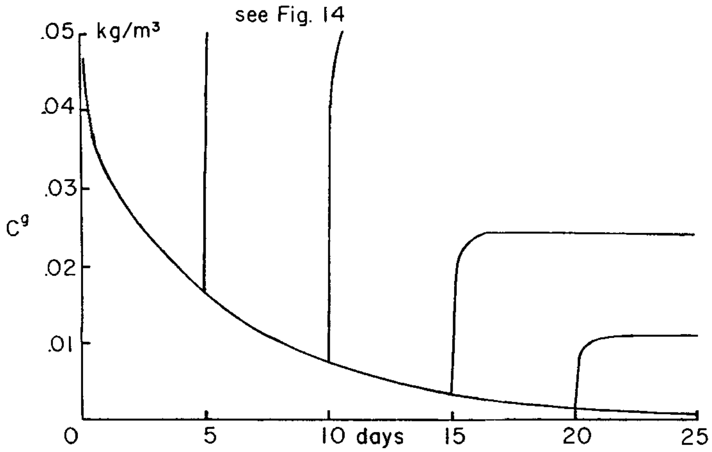

FIG. 13 Plots of vapor phase VOC concentration just within the lower outside edge of the zone of contamination; rebound after well shutdown. Gas flow rate = 10 cfm; other parameters as in Table 1. The curves branching off from the descending curve show VOC concentration rebound after periods of well operation of 5, 10, 15, and 20 days. The rebound curves which are cut off are shown at a larger scale in Fig. 14.

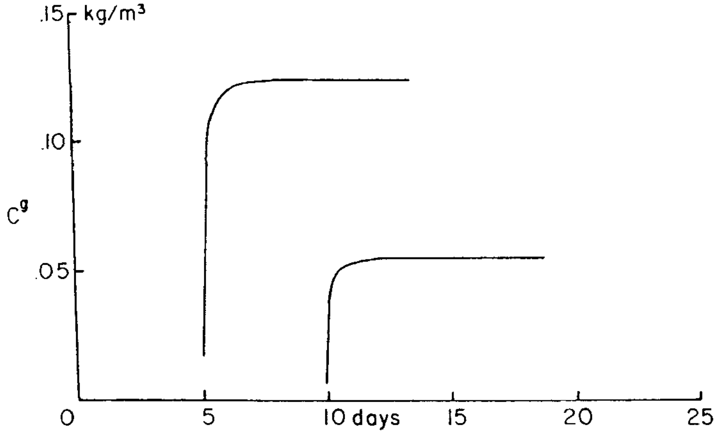

FIG. 14 Plots of vapor phase VOC concentration just within the lower outside edge of the zone of contamination; rebound after well shutdown. Gas flow rate = 10 cfm; other parameters as in Table 1. These plots show the rebound curves which are cut off in Fig. 13; these are the curves resulting when well operation is stopped after 5 or 10 days.

plots in Fig. 12 show soil gas VOC concentration rebound in a volume element immediately adjacent to the well, which is screened 2.5 m below the bottom of the contaminated zone. After 5 days of operation we see a negative rebound, as VOC mobilized from the contaminated zone and drawn to this volume element by advection then diffuses from the gas phase into the virtually uncontaminated porous medium in the immediate vicinity of the well. After longer periods of operation, sufficient VOC has diffused into the porous medium at this location so that normal (positive) rebound is observed. The magnitude of the rebound at this location (outside of the initially contaminated zone) is in all cases quite small, however.

Figures 13 and 14 show soil gas VOC concentration rebound at a point lying just inside the lower outer boundary of the contaminated zone. Rebounds here are always positive, and they are much larger than those observed in Fig. 12 up to the point in time at which remediation is nearly complete.

The results described above lead us to the following conclusions.

- First, this model yields qualitatively the same sort of "tailing" of SVE cleanups as has been seen with our earlier distributed diffusion models. Cleanup rates are initially rapid but drop off markedly as diffusion limitations become controlling.
- Second, it is probably unimportant precisely which SVE model is used to describe SVE, provided that the model includes some sort of distrib-

uted diffusion picture for diffusion mass transport of VOC. The conclusions supported by our earlier distributed diffusion models are also supported by this model.

- Third, SVE remediation will be slowed down, possibly quite substantially, if the soil gas is ''short-circuited'' to the vacuum well through a network of high-permeability channels. This dictates that VOC in the regions of lower permeability must diffuse out to the high permeability channels before it can be removed by the advecting gas.
- Fourth, absence of significant soil gas VOC concentration rebound is an indicator of complete or nearly complete cleanup only if the soil gas sample is taken from a point located in the zone which was actually contaminated. As seen in our results here, rebound can actually be negative outside the zone of contamination while there is still a great deal of VOC remaining at the site. This result should be valid for all of our distributed diffusion models.

ACKNOWLEDGMENTS

D.J.W. is greatly indebted to the University of Malaga for its hospitality and the use of its facilities, to Dr. J. J. Rodriguez-Jimenez for making his visit to Malaga possible, to Vanderbilt University for financial support during his leave, and to the Spanish Government (DGICYT) for a fellowship in support of this work. J.M.R.M. and C.G.L. are indebted to the Spanish Government (CICYT) for financial support through Project AMB 94-0527.

REFERENCES

1. T. A. Pedersen and J. T. Curtis, *Soil Vapor Extraction Technology Reference Handbook*, Risk Reduction Engineering Laboratory, US EPA Report EPA/540/2-91/003, 1991.
2. J. P. Stumbar and J. Rawe, *Guide for Conducting Treatability Studies under CERCLA: Soil Vapor Extraction Interim Guidance*, US EPA Report EPA/540/2-91/019A, 1991.
3. D. J. Wilson and A. N. Clarke, ''Soil Vapor Extraction,'' in *Hazardous Waste Site Soil Remediation: Theory and Application of Innovative Technologies* (D. J. Wilson and A. N. Clarke, Eds.), Dekker, New York, 1993, p. 171.
4. M. D. LaGrega, P. L. Buckingham, and J. C. Evans, *Hazardous Waste Management*, McGraw-Hill, New York, 1994, p. 460.
5. J. M. Rodríguez-Maroto, D. J. Wilson, and C. Gómez-Lahoz, ''Soil Cleanup by In-Situ Aeration. XXI. Effects of Desorption Rates and Equilibria on Remediation Rates,'' *Sep. Sci. Technol.*, *30*, 521 (1955).
6. D. C. DiGiulio, *Evaluation of Soil Venting Application*, US EPA Report EPA/540/S-92/004, April 1992.
7. D. C. DiGiulio, J. S. Cho, R. R. Dupont, and M. W. Kemblowski, ''Conducting Field Tests for Evaluation of Soil Vacuum Extraction Application,'' in *Proceedings, 4th*

National Outdoor Action Conference on Aquifer Restoration, Ground Water Monitoring and Geophysical Methods, Las Vegas, NV, May 14–17, 1990, p. 587.

8. C. Gómez-Lahoz, J. M. Rodríguez-Maroto, and D. J. Wilson, "Soil Cleanup by In-Situ Aeration. XVII. Field Scale Model with Distributed Diffusion," *Sep. Sci. Technol.*, *29*, 1251 (1994).
9. J. M. Rodríguez-Maroto, C. Gómez-Lahoz, and D. J. Wilson, "Soil Cleanup by In-Situ Aeration. XVIII. Field Scale Model with Diffusion from Clay Structures," *Ibid.*, *29*, 1367 (1994).
10. D. J. Wilson, J. M. Rodríguez-Maroto, and C. Gómez-Lahoz, "Soil Cleanup by In-Situ Aeration. XIX. Effects of Spill Age on Soil Vapor Extraction Remediation Rates," *Ibid.*, *29*, 1645 (1994).
11. C. Gómez-Lahoz, J. M. Rodríguez-Maroto, and D. J. Wilson, "Soil Cleanup by In-Situ Aeration. XXII. Impact of Natural Soil Organic Matter on Cleanup Rates," *Ibid.*, *30*, 659 (1995).
12. D. J. Wilson, C. Gómez-Lahoz, and J. M. Rodríguez-Maroto, "Groundwater Cleanup by In-Situ Sparging. VIII. Effect of Air Channeling on Dissolved VOC Removal Efficiency," *Ibid.*, *29*, 2389 (1994).

Received by editor October 24, 1994